Konstantin I. Popov · Stojan S. Djokić
Nebojša D. Nikolić · Vladimir D. Jović

Morphology of Electrochemically and Chemically Deposited Metals

Springer

Morphology of Electrochemically and Chemically Deposited Metals

Konstantin I. Popov • Stojan S. Djokić
Nebojša D. Nikolić • Vladimir D. Jović

Morphology of Electrochemically and Chemically Deposited Metals

Springer

Konstantin I. Popov
University of Belgrade
Belgrade, Serbia

Stojan S. Djokić
Elchem Consulting Ltd.
Edmonton, Alberta, Canada

Nebojša D. Nikolić
ICTM- Institute of Electrochemistry
University of Belgrade
Belgrade, Serbia

Vladimir D. Jović
Institute for Multidisciplinary Research
University of Belgrade
Belgrade, Serbia

ISBN 978-3-319-26071-6 ISBN 978-3-319-26073-0 (eBook)
DOI 10.1007/978-3-319-26073-0

Library of Congress Control Number: 2016932404

Printed on acid-free paper

This Springer imprint is published by Springer Nature
The registered company is Springer International Publishing AG Switzerland

Preface

The aim of this book is to bring to scientists, researchers, engineers, and students the newest achievements in electrochemically and chemically deposited metals and alloys. This book is to some degree a continuation of our former book *Fundamental Aspects of Electrometallurgy*, although there are significant differences. More particularly, this book is devoted to the surface morphology of deposited metals and/or alloys and offers an in-depth analysis of the influence of the parameters of electrodeposition or chemical deposition of metals and alloys, which could lead to technological advances in industrial settings worldwide. As such, the proposed book may equally attract attention from those working in electrometallurgical or electroplating plants and from members of research departments in industry or academia.

The surface morphology of electrochemically deposited metals and alloys is a very important property and thus may significantly influence their potential applications. Conditions of electrochemical deposition such as electrolyte composition, pH, temperature, stirring, time, deposition overpotential, and current density determine the surface morphology.

The morphology of electrodeposited metals is usually analyzed on the basis of the exchange current density and overpotential for hydrogen evolution. When electrodeposition of metals is characterized by *very large* exchange current densities, at lower overpotentials individual grains or boulders are formed, while at higher overpotentials formation of dendrites takes place. In the case of *large* exchange current densities, spongy deposits and dendrites are produced at lower or higher overpotentials, respectively. Finally, during electrodeposition characterized by *medium and low* exchange current densities, compact deposits are obtained at low overpotentials, while dendrites or spongy deposits are formed at high overpotentials.

A proper analysis of the polarization curves in correlation with the surface morphology could contribute to very important conclusions useful for technological operations in order to produce a metal deposit with the desired properties. Electrodeposition of metals at low overpotentials proceeds under ohmic

control and at higher overpotentials under diffusion control when the process is characterized by the *extremely large* exchange current densities. In the ohmic control regime, granular or regular crystals are deposited, while under diffusion control, different shapes of dendrites are formed. When the electrodeposition of metals is characterized by *large* exchange current densities, diffusion control is observed in the whole range of overpotentials. Therefore, spongy deposits are formed at lower and dendrites at higher overpotentials. For metals where electrodeposition is characterized by *medium or low* exchange current densities, the process proceeds under activation control at low overpotentials. Activation-controlled electrodeposition produces large grains of metal with well-defined crystal shapes. This is observed for overpotentials in the regions of the Tafel linearity. For overpotentials larger than those consistent with Tafel linearity and smaller than those determining the limiting diffusion current density plateau (the mixed activation–diffusion control), the surface morphology is influenced by mass transfer. Compact or uniform deposits of metals are obtained under these conditions. Formation of dendrites is observed at overpotentials inside the plateau of the limiting diffusion current density. For metals where electrodeposition is characterized by *medium and low* exchange current densities, the shapes of dendrites are very different than those produced for metals where the electrodeposition is characterized by the *extremely large or large* exchange current densities. This observation raises many further questions from the fundamental point of view of material science in conjunction with electrochemistry and opens a new window for future studies.

Vigorous hydrogen evolution changes hydrodynamic conditions in the near-electrode layer. In this way the presence of significant hydrogen evolution may strongly affect the morphology of metal deposits. The typical structure obtained in the presence of vigorous hydrogen evolution is honeycomb-like, with holes or pores formed from detached hydrogen bubbles and surrounded by cauliflower-like agglomerates of metal grains. Complexing agents and additives (organic or inorganic) present in the electroplating solutions may also strongly affect the morphology of deposits. The difference in the morphology of electrodeposited metals relative to the one obtained by the electrodepositions from simple salt solutions is caused by the change of the kinetic parameters of electrodeposition due to the effect of additives or complexing agents. The deposition of compact metals and alloys, bright galvanic coatings, and dispersed and powdered precipitates is discussed in detail. Also, the effects of periodically changing currents and/or potentials during the electrodeposition on the morphology and related properties of deposits are thoroughly presented in this book.

All the remarks mentioned above are applicable as well to the electrodeposition of alloys. Using Brenner's classification of alloy electrodeposition, e.g., equilibrium, regular, anomalous, etc., all existing combinations of deposition parameters and their influence on the alloy morphology are analyzed. Interestingly, certain features, which are not recognized in the electrodeposition of pure metals, are observed in the alloy deposition processes. An example includes the *spatiotemporal structures*, which is discussed in this book.

Chemically deposited metals and alloys from aqueous solutions have been significantly less studied than their electrodeposition counterparts. Both chemical deposition, or as frequently termed in the literature *electroless* deposition, and electrodeposition are charge transfer processes and as such can be considered as *electrochemical*. Practically, all metals and/or alloys that can be electrodeposited from aqueous solutions can be deposited by the electroless means using appropriate reducing agents. Electroless deposition of various metals has been widely used in industry since the 1950s. Metals of interest include Ni, Cu, Ag, Au, Pd, and Co. Many alloys of these metals find applications in different industries. Both galvanic and autocatalytic types of electroless deposition in relation with the surface morphology are analyzed in this book.

The electrodeposition portion of this book is written by Popov, Nikolić, and Jović. Chapters 1, 2, and 3 are written by Popov and Nikolić, Chap. 4 is written by Popov, Chap. 5 is written by Nikolić, Chap. 6 is written by Nikolić and Popov, and Chaps. 7 and 8 are written by Jović. The chapter related to the chemical deposition is written by S. Djokić. Chapters 1, 2, 3, 4, 5, 6, 7, and 8 of this book are based on classical studies performed at the Department of Physical Chemistry and Electrochemistry at the Faculty of Technology and Metallurgy, University of Belgrade; Department of Electrochemistry at the Institute of Chemistry, Technology and Metallurgy (ICTM), University of Belgrade; and at the Institute for Multidisciplinary Research, University of Belgrade, Serbia. K. I. Popov, N.D. Nikolić, and V.D. Jović would like to acknowledge contributions and inspiration by Professor A.R. Despić who initiated research in the area of electrodeposition at the University of Belgrade. Popov and Nikolić (Chaps. 1, 2, 3, 4, 5, and 6) are thankful for help from their colleagues Professors M.D. Maksimović, M.G. Pavlović, N.V. Krstajić, B.N. Grgur, P.M. Živković, S.K. Zečević, and B.J. Lazarević. Also they acknowledge contributions from Drs R.M Stevanović, S.M Pešić, Z. Rakočević, Lj.J. Pavlović, G. Branković, V.M. Maksimović, and S.B. Krstić, as well as from numerous colleagues and students who participated in their research.

V.D. Jović (Chaps. 7 and 8) is thankful to U.Č. Lačnjevac and B.M. Jović from the Institute for Multidisciplinary Research University of Belgrade, Serbia, for contributions in the published chapters in *Modern Aspects of Electrochemistry* series. He further expresses his gratitude to Prof. Ivan Krastev, Institute of Physical Chemistry, Bulgarian Academy of Science, for providing necessary literature and explanation of specific structural phenomena in electrodeposition of alloys, given in Sect. 2.3 of Chap. 7. Popov, Nikolić, and Jović are also indebted to the Ministry of Education, Science and Technological Development of the Republic of Serbia, for the financial support of this work.

Djokić is very thankful to many colleagues across the globe (Europe, North America, China, and India) for inspiring him to further investigate chemical deposition processes. Special thanks go to all of his students, clients, and his family for the establishment of a few electroless processes in industry. Further, Djokić expresses his thanks to Dr. Kenneth Howell of Springer for many very helpful advice during the preparation of this book. As well, Djokić acknowledges the help

of Ms. Marion Pritchard and Ms. Nada Djokić (both from University of Alberta, Canada) for their unselfish help in the preparation of this manuscript.

We hope that the book will be of a particular interest to the individuals or groups dealing with electrochemistry of metals or more specifically with the electrodeposition phenomena in relation with the surface morphology. The research departments in the automotive, aerospace, electronics, energy device, and perhaps in the biomedical fields may find this book as a very useful source in developments of their future programs. Professors and students in the university settings worldwide, when learning, investigating, or lecturing various electrodeposition processes at both undergraduate or graduate levels, will find this book as a very valuable source for their courses and/or projects. We believe that for the university environments, the book can be attractive to the engineering students. Perhaps, chemistry or physics students will find the book as a very useful source in their studies.

Belgrade, Serbia — Konstantin I. Popov
Edmonton, Alberta, Canada — Stojan S. Djokić
Belgrade, Serbia — Nebojša D. Nikolić
Belgrade, Serbia — Vladimir D. Jović
August, 2015

Contents

Short Biographies

Konstantin I. Popov Professor Konstantin I. Popov received his BSc, MSc, and PhD degrees in the field of electrochemical science, from the Faculty of Technology and Metallurgy, University of Belgrade, Serbia. He joined the Faculty of Technology and Metallurgy as a teaching assistant and advanced to the position of full professor of electrometallurgy at the Department of Physical Chemistry and Electrochemistry, at the same institution. At the same time, Professor Popov closely collaborated with the Institute of Chemistry, Technology and Metallurgy (ICTM), Department of Electrochemistry, University of Belgrade, Serbia. During his rich academic carrier, Professor Popov has published over 230 research papers, twelve book chapters, and coauthored the book *Fundamental Aspects of Electrometallurgy*. In addition, Popov has published several textbooks devoted to the electrochemistry/electrometallurgy fields in the Serbian language which are used by the university students and professionals there. He had numerous presentations, including invited lectures, at national and international conferences. Professor Popov successfully supervised more than 80 students in their BSc, MSc, and PhD research studies. The main scientific interests of Professor Popov include various fundamental and applied aspects of electrochemical deposition and dissolution of metals, constant and periodically changing regimes of electrolysis, production and characterization of metal powders by electrolysis, the current density distribution effects, bright coatings, and open porous electrodes (the honeycomb-like structures). Professor Popov is a member of the Serbian Chemical Society and Serbian Society of Corrosion and Materials Protection. He is a recipient of several national awards, including Medal of Serbian Chemical Society for enduring and outstanding contributions to science. Currently, Professor Popov is an emeritus scientist of the Republic of Serbia.

Stojan S. Djokić Dr. Djokić obtained his BSc degree in chemical engineering/analytical chemistry from the University of Belgrade, Yugoslavia. He holds an MSc in electrochemical energy conversion and a PhD in electrochemistry/materials science from the University of Belgrade. At the University of Ottawa, as a research

fellow, he has successfully collaborated with Alcan International Ltd. in the field of molten salts electrochemistry. He was a senior scientist/electrochemist at Sherritt Inc., Westaim Corporation, Westaim Ambeon, Superior MicroPowders, etc., working on various projects related to electronics, automotive/aerospace, corrosion, and metallurgical and biomedical applications. Dr. Djokić has published more than 90 papers including seven book chapters and coauthored a book *Fundamental Aspects of Electrometallurgy,* and he has edited four volumes of *Modern Aspects of Electrochemistry*. He holds eight US patents. Dr. Djokić is an active member of the Electrochemical Society, and he has successfully organized and chaired several international symposiums. He is as well a registered professional engineer with the APEGA. Stojan's professional experience covers both industrial and academic environments within Europe, North America, and China in the fields of electrochemistry, electrometallurgy, polymeric composite materials, biomaterials, materials science, and analytical chemistry. Dr. Djokić has developed several processes and materials which are currently used in industry worldwide. His current interests include electroless and electrodeposition, kinetics, disinfectants, electronic materials, and biomaterials used as infection-resistant surfaces or in immunodiagnostics. Currently, Dr. Djokić is the director of Elchem Consulting Ltd. and an adjunct professor of chemical and materials engineering at the University of Alberta.

Nebojša D. Nikolić Dr. Nebojša D. Nikolić graduated from the Faculty of Technology and Metallurgy, University of Belgrade, Serbia, where he earned his BSc, MSc, and PhD degrees in the field of electrochemical science. Presently, he is a senior research scientist (full research professor) at the Institute of Chemistry, Technology and Metallurgy (ICTM), Department of Electrochemistry, University of Belgrade, Serbia. Dr. Nikolić had an intensive scientific collaboration with Laboratorio de Fisica de Sistemas Pequnos y Nanotechnologia, CSIC, Madrid, Spain, and Departamento de Fisica, Universidade Federal de Santa Catarina (UFSC), Florianopolis–Santa Catarina, Brazil. The main research interests of Dr. Nikolić encompass various aspects of electrochemical metal deposition and dissolution, including bright coating formation, electrochemical production of metal powders, application of periodically changing regimes of electrolysis, and other related phenomena. A special topic of his investigation involves the synthesis and characterization of open porous structures of copper (the honeycomb-like deposits), using constant and periodically changing regimes of electrolysis. Dr. Nikolić has been author or coauthor of ten chapters in relevant books (including eight chapters in *Modern Aspects of Electrochemistry*) as well as 102 original scientific papers. In addition, he had 76 presentations, including invited lectures, at national and international conferences. He is a member of the ISE (International Society of Electrochemistry), Serbian Chemical Society, Serbian Society of Corrosion and Materials Protection, and Association of the Chemical Engineers of Serbia (AChE).

Vladimir D. Jović Dr. Vladimir D. Jović obtained his BSc, MSc, and PhD in the field of electrochemical science and technology from the University of Belgrade, Serbia. He has an extensive academic experience at the University of Belgrade

working as a researcher at the Institute of Technical Sciences of the Serbian Academy of Science and Arts and Institute for Multidisciplinary Research, University of Belgrade, Serbia. As well, Dr. Jović was a guest scientist at the National Institute of Standards and Technology, Materials Science and Engineering Laboratory, Gaithersburg, MD, USA, and a research associate at the Department of Materials Engineering, Drexel University, Philadelphia, USA. His main interests in the field of electrochemistry include the underpotential deposition of Pb, Tl, and Cd onto Ag and Cu single crystals from aqueous solutions; anion adsorption onto Ag and Cu single crystals from aqueous solutions; UPD of Al onto Cu single crystals from room-temperature AlCl3–MeEtimCl molten salt; characterization of electrodeposited binary alloys by electrochemical ALSV technique; electrodeposition of metals, powders, alloys, and composite structures; electrochemistry of MAX phases; and electrodeposited catalysts for industrial electrolysis. Dr. Jović published more than 130 scientific papers (including chapters), 3 patents, and over 200 poster presentations and was an invited speaker on numerous international occasions. Currently, Dr. Jović is a retired senior research fellow from the Institute for the Multidisciplinary Research, University of Belgrade, Serbia.

Chapter 1
The Cathodic Polarization Curves in Electrodeposition of Metals

1.1 Introduction

Morphology is probably the most important property of electrodeposited metals. It depends mainly on the kinetic parameters of the deposition process and on the deposition overpotential or current density. The morphology of an electrodeposited metal also depends on the deposition time until the deposit has attained its final form.

Morphology of electrodeposited metal strongly depends on the nature of metals, and electrodeposition processes are usually classified in the dependence of the exchange current density of deposition process [1]. For example, the individual grains or boulders formed at lower overpotentials and dendrites at higher ones are characteristics of the electrodeposition processes characterized by very large exchange current densities. Formation of spongy deposits at lower overpotentials and dendrites at higher ones is a characteristic of the electrodeposition processes characterized by large exchange current densities. Finally, compact deposits are obtained at lower overpotentials, while both dendritic and spongy-dendritic deposits are formed at higher overpotentials during electrodeposition of metals characterized by medium and low exchange current densities.

Obviously, morphology of metal electrodeposits depends on the type of control of the electrodeposition process. For example, the activation-controlled electrodeposition of copper produces large grains with relatively well-defined crystal shapes. This happens at overpotentials belonging to the region of the Tafel linearity [2, 3]. At overpotentials that are between the end of the Tafel linearity and the beginning of the limiting diffusion current density plateau (the mixed activation–diffusion control), morphological forms are influenced by the mass transfer conditions, and large grains are not formed [4, 5]. Dendrites are formed at overpotentials inside the plateau of the limiting diffusion current density and at the higher ones at which there is no hydrogen evolution or it is not enough to affect hydrodynamic conditions in the near-electrode layer [6, 7]. The above consideration is valid for all

K.I. Popov et al., *Morphology of Electrochemically and Chemically Deposited Metals*, DOI 10.1007/978-3-319-26073-0_1

electrodeposition processes characterized by medium and low values of the exchange current density in the absence of the noticeable hydrogen evolution reaction [7]. In the presence of strong hydrogen evolution, the honeycomb-like deposits are formed [7].

On the other hand, formation of spongy deposits at the lower, and dendrites at the higher, overpotentials was explained by long-standing assumption that the electrodeposition processes characterized by large values of the exchange current density are diffusion controlled at all overpotentials [8]. However, formation of individual grains or granules at low overpotentials was not possible to explain by this assumption. Recently, it was discussed [9] the linear dependence of current density on the overpotential for the fast electrochemical processes, and it was shown that this linear dependence can be ascribed to the ohmic control of the electrodeposition process [10–13].

There is a close correlation between the morphology of metal electrodeposits and the electrodeposition process control. Besides, the shape of the polarization curve depends also on the electrodeposition process control. Hence, it can be expected that the morphology of deposits can be correlated with the shape of the polarization curves. This chapter introduces the basic correlations between polarization and morphological characteristics of metal deposits.

1.2 Polarization Curves for the Case of Massive Active Cathodes

1.2.1 Polarization Curves Without Included Ohmic Potential Drop

1.2.1.1 Concentration Dependence of the Exchange Current Density Is Not Taken into Account

The general form of current density–overpotential relationship in electrodeposition of metals for the reaction

$$\mathrm{Ox} + n\mathrm{e}^- \rightleftarrows \mathrm{Red} \tag{1.1}$$

taking cathodic current density and overpotential as positive, is given by

$$i = i_0 \left[\left(\frac{a_\mathrm{i}^\mathrm{O}}{a_\mathrm{e}^\mathrm{O}} \right) f_\mathrm{c} - \left(\frac{a_\mathrm{i}^\mathrm{R}}{a_\mathrm{e}^\mathrm{R}} \right) f_\mathrm{a} \right] \tag{1.2}$$

where i_0 is the exchange current density and a_i is the activity of the oxidized (Ox) or reduced (Red) state at a current density i and a_e is the activity in the equilibrium state [14].

On the other hand,

$$f_{\mathrm{c}} = \exp\left(\frac{\alpha_{\mathrm{c}} F\eta}{RT}\right) = \exp\left(\frac{2.3}{b_{\mathrm{c}}}\eta\right) \tag{1.3}$$

and

$$f_{\mathrm{a}} = \exp\left(\frac{-\alpha_{\mathrm{a}} F\eta}{RT}\right) = \exp\left(\frac{-2.3}{b_{\mathrm{a}}}\eta\right) \tag{1.4}$$

where α_{c} and α_{a} are the cathodic and anodic transfer coefficient, b_{c} and b_{a} are corresponding Tafel slopes, and η is the overpotential, and

$$b_{\mathrm{c}} = \frac{2.3RT}{\alpha_{\mathrm{c}} F} \tag{1.5}$$

and

$$b_{\mathrm{a}} = \frac{2.3RT}{\alpha_{\mathrm{a}} F} \tag{1.6}$$

where R is gas constant, T is temperature, and F is Faraday constant.

The ratio of the activities for the cathodic reaction may be written as

$$\frac{a_{\mathrm{i}}^{\mathrm{O}}}{a_{\mathrm{e}}^{\mathrm{O}}} = 1 - \frac{i}{i_{\mathrm{L}}} \tag{1.7}$$

where i_{L} is the limiting diffusion current density, and for the reverse anodic reaction as [14]

$$\frac{a_{\mathrm{i}}^{\mathrm{R}}}{a_{\mathrm{e}}^{\mathrm{R}}} = \exp\frac{2\gamma V}{RTr_{\mathrm{el}}} \tag{1.8}$$

taking into account the Kelvin term which becomes appreciable at low values of electrode radii [15]. In Eq. (1.8), γ is the interfacial energy between metal and solution, V is the molar volume of the electrodeposited metal, and r_{el} is the radius of the spherical electrode. Equation (1.8) is valid for two electron reactions [14], while the other possibilities are discussed in Ref. [16].

For a spherical electrode, Eq. (1.2) can be written as

$$i_{\mathrm{spher}} = i_0\left[\left(1 - \frac{i}{i_{\mathrm{L,\,spher}}}\right)f_{\mathrm{c}} - f_{\mathrm{a}}\exp\left(\frac{2\gamma V}{RTr_{\mathrm{el}}}\right)\right] \tag{1.9}$$

or

$$i_{\text{spher}} = \frac{i_0\left[f_c - f_a \exp\left(\frac{2\gamma V}{RTr_{el}}\right)\right]}{1 + \frac{i_0 f_c}{i_{L,\text{spher}}}} \tag{1.10}$$

where

$$i_{L,\text{spher}} = \frac{nFDC_0}{r_{el}} \tag{1.11}$$

and n is the number of electrons involved in the electrode reaction, C_0 is the bulk concentration, and D is the coefficient of diffusion of a depositing ions. A somewhat modified Eq. (1.10) is necessary for an understanding of electrodeposition on the tip of dendrites inside the diffusion layer of a macroelectrode (see Chap. 2) and in the case of electrodeposition at a periodically changing rate (see Chap. 4) [1, 17].

For sufficiently large r_{el} to make surface energy term negligible, Eq. (1.10) can be rewritten in the form:

$$i_{\text{spher}} = \frac{i_0(f_c - f_a)}{1 + \frac{i_0 f_c}{i_{L,\text{spher}}}} \tag{1.12.}$$

For flat electrodes and sufficiently large spherical electrodes, Eq. (1.10) becomes

$$i = \frac{i_0(f_c - f_a)}{1 + \frac{i_0 f_c}{i_L}} \tag{1.13}$$

where

$$i_L = \frac{nFDC_0}{\delta} \tag{1.14}$$

and δ is the diffusion layer thickness.

1.2.1.2 Concentration Dependence of the Exchange Current Density Is Taken into Account

In this case, the current density is given by

$$i = i_{0,s}(f_c - f_a) \tag{1.15}$$

where $i_{0,s}$ is the exchange current density on the electrode surface at current density i, being determined by Eq. (1.16) [18]:

$$i_{0,\mathrm{s}} = \left(\frac{C_\mathrm{s}}{C_0}\right)^{\xi} i_0 \tag{1.16}$$

where C_s is the surface concentration, i_0 is the exchange current density for a surface concentration C_0 equal to the one in the bulk, and $i_{0,\mathrm{s}}$ is the exchange current density for a surface concentration C_s, and

$$\xi = \frac{\mathrm{d}\log i_0}{\mathrm{d}\log C_0} \tag{1.17}$$

Using relation

$$\frac{C_\mathrm{s}}{C_0} = 1 - \frac{i}{i_\mathrm{L}} \tag{1.18}$$

Eq. (1.15) can be rewritten in the form:

$$i = i_0\left(1 - \frac{i}{i_\mathrm{L}}\right)^{\xi}(f_\mathrm{c} - f_\mathrm{a}) \tag{1.19}$$

or, for $\zeta = 1$, after rearranging

$$i = \frac{i_0(f_\mathrm{c} - f_\mathrm{a})}{1 + \frac{i_0(f_\mathrm{c} - f_\mathrm{a})}{i_\mathrm{L}}} \tag{1.20}$$

It is necessary to note that Eq. (1.20) is an approximation because the value of ζ is lower than unity. This approximation is widely used in qualitative discussions, because it permits the simple mathematical treatment of electrochemical processes with relatively small errors and with clear physical meaning. If ζ different than unity is included in the derivation of the general polarization curve equation, simple analytical solutions are not available and numerical solutions are required.

1.2.1.3 Comparison of Eqs. (1.13) and (1.20) for Different Exchange Current Density to the Limiting Diffusion Current Density Ratios

Equations (1.13) and (1.20) are compared taking $i_0/i_\mathrm{L} = 100$, 10, 1, 0.1, and 0.01. $f_\mathrm{c} = 10^{\frac{\eta}{120}}$ and $f_\mathrm{a} = 10^{-\frac{\eta}{120}}$ and the diagrams presented in Fig. 1.1 are obtained by digital simulation. It can be seen that for $i_0/i_\mathrm{L} \leq 1$, diagrams computed using Eqs. (1.13) and (1.20) are the same.

At larger values of i_0/i_L ratio, the polarization curves calculated by Eq. (1.13) are the same as follows from Eq. (1.13) when $i_0/i_\mathrm{L} \to \infty$, for $f_\mathrm{c} > f_\mathrm{a}$. On the other

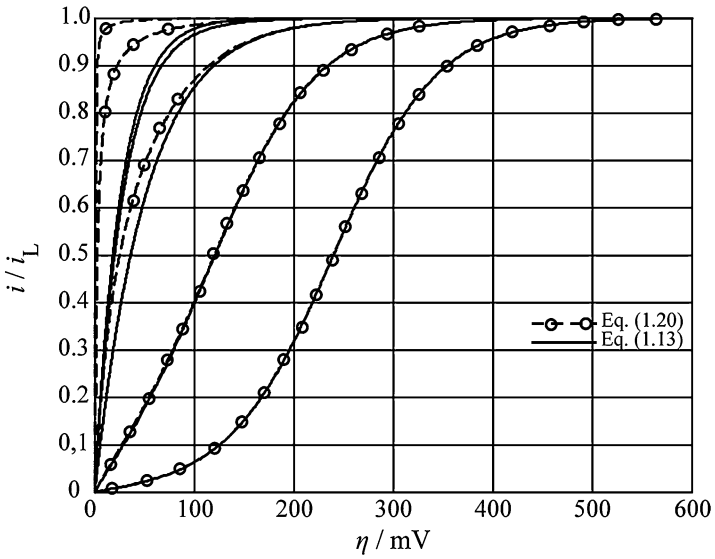

Fig. 1.1 The comparison of polarization curves calculated using Eqs. (1.13) and (1.20). From left to right side of diagram, i_0/i_L ratio corresponds to 100, 10, 1, 0.1, and 0.01, respectively; $f_c = 10^{\frac{\eta}{120}}$, and $f_a = 10^{-\frac{\eta}{120}}$ (Reprinted from Ref. [19] with permission from Elsevier and Ref. [9] with kind permission from Springer)

hand, the polarization curves calculated using Eq. (1.20) under the same conditions become

$$i \cong i_L \tag{1.21}$$

at all overpotentials for $i_0/i_L \to \infty$. It can be seen from Fig. 1.1 that the increase of the value of i_0/i_L ratio leads to the decrease of the electrochemical overpotential. The activation part of overpotential is lost at i_0/i_L values larger than 10, while both activation and diffusion overpotential vanish at i_0/i_L values larger than 100 (Fig. 1.1). In the second case, the ohmic-controlled electrochemical reaction can occur (see Sects. 1.2.1.5 and 1.2.2.2).

1.2.1.4 The Approximations for $i_0/i_L << 1$

Although Eqs. (1.13) and (1.20) are generally valid, it is more convenient to use some approximative relations derived from them [1]. For a flat surface, if

$$f_c > f_a \text{and } \frac{i_0 f_c}{i_L} << 1 \tag{1.22}$$

Eqs. (1.13) and (1.20) can be rewritten in the form:

$$i = i_0(f_c - f_a) \tag{1.23}$$

which becomes

$$i = i_0 \frac{nF}{RT}\eta \tag{1.24}$$

at very low overpotentials by expanding the exponential terms in Eq. (1.23) and retaining the two terms of expansion of each exponential terms, if

$$\alpha_c = \beta n \tag{1.25}$$

and

$$\alpha_a = (1 - \beta)n \tag{1.26}$$

where β is the symmetry factor.

When

$$f_c >> f_a \text{ and } \frac{i_0 f_c}{i_L} << 1 \tag{1.27}$$

the relation

$$i = i_0 f_c \tag{1.28}$$

or

$$\eta = \frac{b_c}{2.3}\ln\frac{i}{i_0} \tag{1.29}$$

is valid.

If $f_c >> f_a$, Eqs. (1.13) and (1.20) become

$$i = \frac{i_0 f_c}{1 + \frac{i_0 f_c}{i_L}} \tag{1.30}$$

or

$$\eta = \frac{b_c}{2.3}\ln\frac{i}{i_0} + \frac{b_c}{2.3}\ln\frac{1}{1 - \frac{i}{i_L}} \tag{1.31}$$

For

$$f_c > f_a \text{ and } \frac{i_0 f_c}{i_L} >> 1 \tag{1.32}$$

Eq. (1.13) can be rewritten in the form:

$$i = i_L\left(1 - \frac{f_a}{f_c}\right) = i_L\left[1 - \exp\left(-\frac{nF\eta}{RT}\right)\right] \tag{1.33}$$

which is valid if Eqs. (1.25) and (1.26) are valid. Finally, if

$$f_c >> f_a \text{ and } \frac{i_0 f_c}{i_L} >> 1 \tag{1.34}$$

Eqs. (1.13) and (1.20) become

$$i = i_L \tag{1.35}$$

The range of validity of Eqs. (1.23), (1.24), (1.28), and (1.29) as well as (1.30), (1.31), and (1.35) can be easily determined from $\eta - \log(i)$ and $\eta - i$ plots in Fig. 1.2. Equations (1.28) and (1.29) are valid from the beginning to the end of Tafel linearity (Tafel line). At lower overpotentials, Eqs. (1.23) and (1.24) are valid,

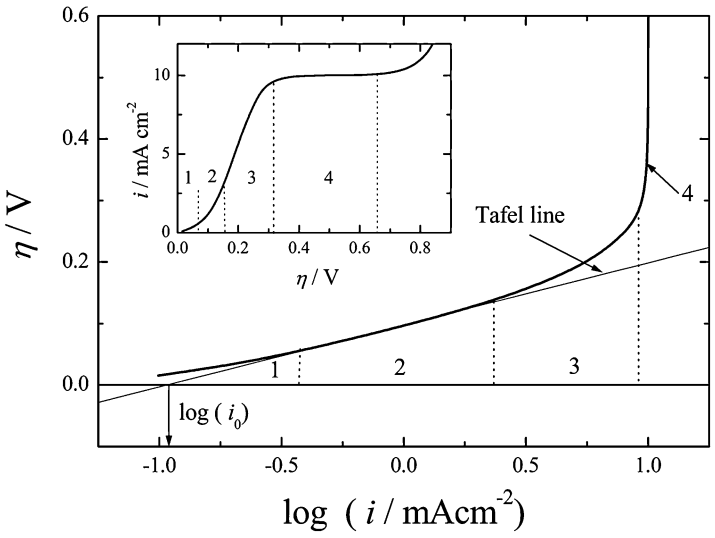

Fig. 1.2 Simulated Tafel plot for the metal deposition ($i_0 = 0.11$ mA cm^{-2}; $b_c = 118$ mV dec^{-1}; $b_a = 40$ mV dec^{-1}; $i_L = 10$ mA cm^{-2}) and range of validity of equation: (*1*) Eqs. (1.23) and (1.24), (*2*) Eqs. (1.28) and (1.29), (*3*) Eqs. (1.30) and (1.31), and (*4*) Eq. (1.35). Insert: polarization curve (Reprinted from Ref. [1] with kind permission from Springer)

while at higher ones, Eqs. (1.30), (1.31), and (1.35) are valid. In Fig. 1.2, the simulated polarization curve for cathodic metal electrodeposition together with the Tafel plot and the range of validity of mentioned equations is shown. Usually, in electrochemistry the marked regions are called (1 and 2) activation-controlled region, (3) mixed activation–diffusion-controlled region, and (4) pure diffusion-controlled region.

1.2.1.5 The Shape of the Calculated Polarization Curves as Function of i_0/i_L Ratio Without Included Ohmic Potential Drop

Using the current density–overpotential relationships and the procedure for the determination of the ohmic potential drop, the polarization curves for electrodeposition processes can be successfully simulated [9, 20].

The current density–overpotential curve equation (Eq. (1.20)), derived by taking the concentration dependence of i_0 into account and the linear dependence of i_0 on the C_s/C_0 ratio, can be rewritten in the form:

$$\frac{i}{i_L} = \frac{\frac{i_0}{i_L}(f_c - f_a)}{1 + \frac{i_0}{i_L}(f_c - f_a)} \tag{1.36}$$

being valid for all i_0/i_L ratios and overpotentials. Because of this, this form will be used in discussion of the effect of the i_0/i_L ratio on the shape of the polarization curves. In Eq. (1.36), i, i_0, i_L, C_s, and C_0 have already mentioned meanings, while f_c and f_a can also be written in the form:

$$f_c = 10^{\frac{\eta}{b_c}} \quad \text{and} \quad f_a = 10^{-\frac{\eta}{b_a}} \tag{1.37}$$

where b_c and b_a are the cathodic and anodic Tafel slopes. Equation (1.36) is modified for use in electrodeposition of metals using the values of the cathodic current density and overpotential as positive. In Eq. (1.36), the ohmic potential drop is not included in the overpotential values. Equation (1.36) is operative if IR error is eliminated by using the electronic devices that distinguish the superfast change in potential that occurs in this IR portion, when the current density is switched on and off from the slower change of the electrode potential itself, where the charging of the interfacial capacitor takes time [20]. In this way, the polarization curves which do not include the ohmic potential drop can be simulated using Eq. (1.36).

The polarization curves without including the ohmic potential drop for different i_0/i_L ratio values for both, one and two electron reactions, are shown in Fig. 1.3 [21]. They are obtained by using Eq. (1.36) for the different i_0/i_L ratios and f_c and f_a values obtained for different η, b_a, and b_c in the dependence of the mechanism of electrodeposition reactions. From Fig. 1.3, it is a clear that these dependencies are similar to each other for the large values of the i_0/i_L ratio and at any low value of overpotential. Because of this, the polarization curves without including the ohmic potential drop are not suitable and, for that reason, will be not treated further.

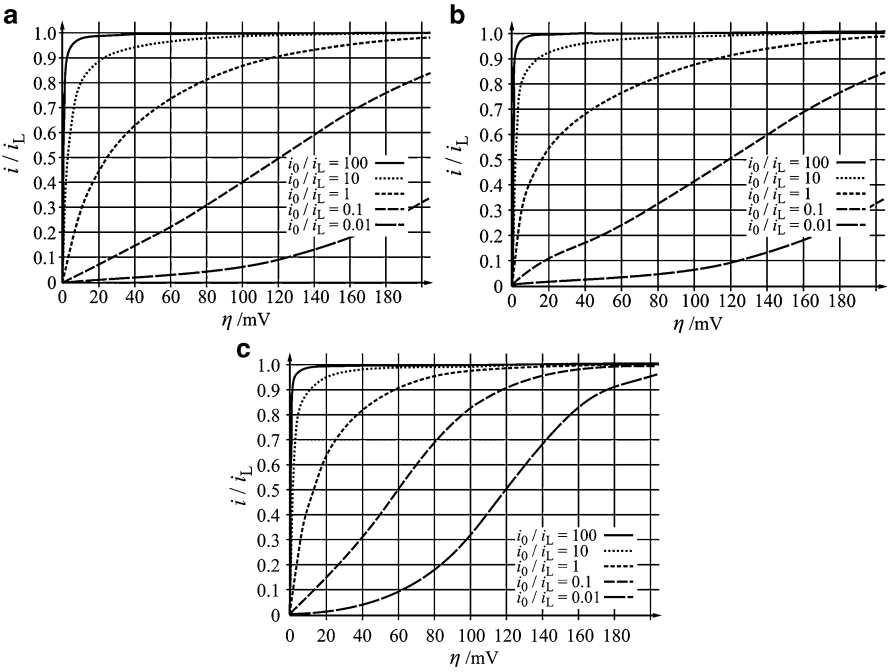

Fig. 1.3 Dependencies $i/i_L - \eta$ calculated using Eqs. (1.36) and (1.37) for the different values of i_0/i_L ratio: (**a**) $b_a = 120$ mV dec^{-1}, $b_c = 120$ mV dec^{-1}; (**b**) $b_a = 40$ mV dec^{-1}, $b_c = 120$ mV dec^{-1}; and (**c**) $b_a = 60$ mV dec^{-1}, $b_c = 60$ mV dec^{-1} (Reprinted from Ref. [21] with permission from the Serbian Chemical Society)

1.2.2 Polarization Curves with Included Ohmic Potential Drop

1.2.2.1 The Structure of Polarization Curves

If IR error is not eliminated, the measured value of overpotential, η_m, includes the ohmic potential drop and it is given by Eq. (1.38) [20]:

$$\eta_m = \eta + i\frac{L_c}{\kappa} \tag{1.38}$$

where i is the current density, L_c is the length of the electrolyte column between the tip of a liquid capillary and the electrode, and κ is the specific conductivity of the electrolyte. The values of i/i_L for selected overpotentials η are obtained using Eq. (1.36), and multiplication with i_L produces the values of i_0. η and i are then substituted in Eq. (1.38), and overpotentials which included ohmic potential, η_m, drop are obtained. Now, $i/i_L - \eta_m$ dependencies can be plotted. Hence, the polarization curves which include ohmic potential drop can be simulated by using Eqs. (1.36) and (1.38) [9].

1.2.2.2 The Shape of the Calculated Polarization Curves as Function of the i_0/i_L Ratios and the Kind of the Electrodeposition Process Control

The shapes of the polarization curves depend strongly on the i_0/i_L ratios. It is obvious that the continuous change of the exchange current density to the limiting diffusion current density ratio for processes of the metal electrodeposition is only possible by the digital simulation. In this way, the relations between i_0/i_L ratios, the shape of polarization curve, and the electrodeposition process control can be established.

The simulated polarization curves which included the ohmic potential drop are shown in Fig. 1.4. They are obtained using the same data as those shown in Fig. 1.3 and for $i_L = 50$ mA cm^{-2}, $L_c = 0.2$ cm, and $\kappa = 0.1$ S cm^{-1}. In all cases, for $i_0/i_L = 100$, there is linear dependence of the current density on overpotential up to $i = 45$ mA cm^{-2} or to $i/i_L \approx 0.9$. In these cases, the overpotential without included ohmic potential drop (see Fig. 1.3) is very low, and the measured overpotential is practically equal to the ohmic potential drop between the working and the reference electrodes. Hence, for $i_0/i_L > 100$, there is the ohmic control of the electrodeposition process. It is obvious that the shape of the linear part of polarization curve does not depend on the mechanism of the electrode reaction.

The polarization curves consist of two parts in the mixed ohmic–diffusion-controlled electrodeposition [12]. The first part corresponds to the ohmic control

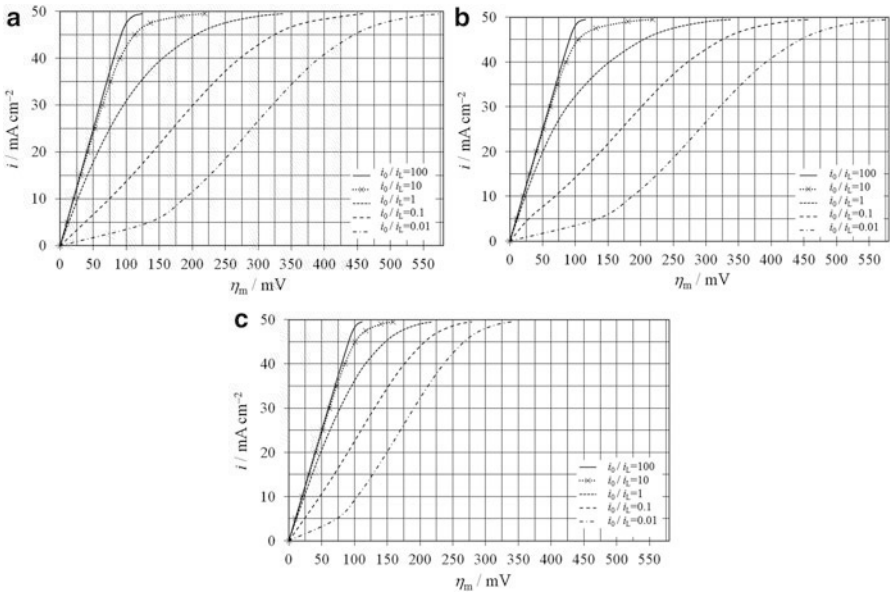

Fig. 1.4 Dependencies $i - \eta_m$ calculated using Eqs. (1.36), (1.37), and (1.38) and the different values of i_0/i_L ratio for $i_L = 50$ mA cm^{-2}, $L_c = 0.2$ cm, and $\kappa = 0.1$ S cm^{-2}: (**a–c**) as in captions in Fig. 1.3 (Reprinted from Ref. [21] with permission from the Serbian Chemical Society)

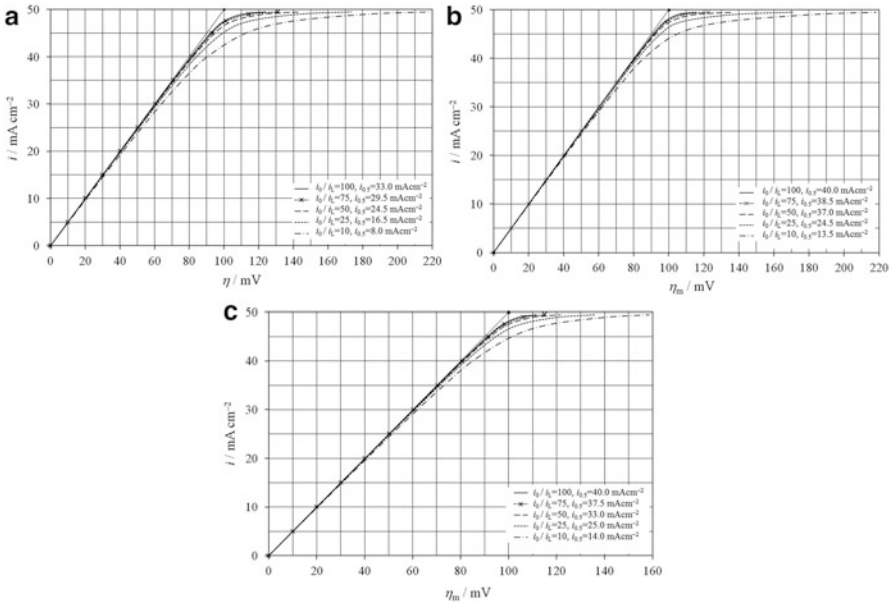

Fig. 1.5 Dependencies $i - \eta_m$ for $10 \leq i_0/i_L \leq 100$ calculated as those in Fig. 1.4. (**a**) $b_a = 120$ mV dec^{-1}, $b_c = 120$ mV dec^{-1}; (**b**) $b_a = 40$ mV dec^{-1}, $b_c = 120$ mV dec^{-1}; and (**c**) $b_a = 60$ mV dec^{-1}, $b_c = 60$ mV dec^{-1} (Reprinted from Ref. [21] with permission of the Serbian Chemical Society)

(it is the linear part), and the second one corresponds to the diffusion control (Fig. 1.5). The length of the ohmic part at the polarization curve decreases with decreasing the i_0/i_L ratio values. Assuming that the diffusion control of the electrodeposition process becomes visible at $\eta_m \geq 0.5$ mV, the values of $i_{0.5}/i_L$ at the end of the linear part of polarization curves are calculated and shown in the function of i_0/i_L ratio in Fig. 1.6 and given in Table 1.1. It can be seen from Fig. 1.6 and Table 1.1 that the linear part of the polarization curve vanishes at $i_0/i_L = 1$. Hence, there is the mixed ohmic–diffusion control in the interval of $1 < i_0/i_L \leq 100$.

At values of i_0/i_L ratio lower than 1, the complete diffusion control of the electrodeposition process arises at all overpotentials. The lower limit of the region of the complete diffusion control can be determined as follows: it is obvious that the convex shape of the polarization curve characterizes the diffusion control of deposition process and the concave one the activation control of deposition process. The i/i_L ratio as function of η is shown in Fig. 1.3 and the i as a function of η_m in Fig. 1.4. In both cases, the convex shape of curves changes in the concave one at approximately $i_0/i_L \sim 0.1$, meaning that the diffusion control changes in the activation one at the beginning of the polarization curve at low η and η_m. At larger overpotentials, the diffusion control occurs. Hence, the diffusion control at all overpotentials appears at $0.1 < i_0/i_L \leq 1$, while the activation control appears at $i_0/i_L \leq 0.1$ at low overpotentials.

It can be seen from Figs. 1.3 and 1.4 that the same conclusion can be derived for the polarization curves with and without included ohmic overpotential drop. The simulated polarization curves with included ohmic drop are calculated using data for